

# Optical Measurement of Cesium Behavior in a Large $H^-$ Ion Source for a Neutral Beam Injector

Katsunori IKEDA, Kenichi NAGAOKA, Yasuhiko TAKEIRI, Katsuyoshi TSUMORI,  
Masaki OSAKABE, Haruhisa NAKANO and Osamu KANEKO

*National Institute for Fusion Science, 322-6 Oroshi, Toki, Gifu 509-5292, Japan*

(Received 25 December 2009 / Accepted 24 March 2010)

Optical emission in a negative hydrogen ion source for the Large Helical Device Neutral Beam Injector (LHD-NBI) has been measured to investigate the behavior of Cs. Two optical sight lines exist parallel to the plasma grid, in the discharge area and in the magnetic filter area near the plasma grid. In the discharge area, the spectrum intensity from  $Cs^+$  ions is considerably increased during 20 s of the beam extraction. This indicates a considerable increase in the  $Cs^+$  density inside the plasma due to the impact of back-streaming  $H^+$  ions. A strong neutral Cs spectrum is observed in the magnetic filter area, where the electron density is lower than in the discharge area. The rate of increase of neutral Cs is much enhanced after  $t = 30$  s, probably because the Cs adsorbed on the cooled region inside the arc chamber evaporates because its temperature increases during the long pulse discharge.

© 2010 The Japan Society of Plasma Science and Nuclear Fusion Research

Keywords: neutral beam injector, negative ion source, cesium, arc discharge

DOI: 10.1585/pfr.5.S2102

## 1. Introduction

Production of negative hydrogen ions ( $H^-$ ) or deuterium ions ( $D^-$ ) is essential for a high-energy neutral beam injector (NBI). Cesium(Cs)-assisted  $H^-$  or  $D^-$  ion sources for NBI have been developed in many facilities [1–3]. The Cs recycling scenario in an  $H^-$  ion source is crucial to the stable operation of NBI systems, especially the future high-power and long-pulse NBI for International Thermonuclear Experimental Reactor (ITER) [4].

At the Large Helical Device (LHD), we have operated  $H^-$  sources for NBI for more than 10 years [5]. We have achieved 16 MW beam injection using three injectors with six negative ion sources, which corresponds to the design power of one injector for ITER-NBI [4], although our negative ion source, which uses filament-arc discharge [6], differs from the RF ion source in the ITER design [7]. Several common concerns apply when using a negative ion source to generate a stable high-power beam: Cs consumption and heat loading from back-streaming positive ions.

Optical emission spectroscopy has been established to investigate Cs behavior and negative ion production inside the RF ion source at IPP Garching [8]. In the Large Helical Device Neutral Beam Injector (LHD-NBI)  $H^-$  ion source, we have reported increasing  $Cs^+$  ions in the arc chamber caused by back-streaming positive ions and changes in the uniformity of the Cs using a view port on the back plate [9, 10]. The behavior of Cs near the plasma grid (PG) and the effects of long beam extraction are very interesting. In

this paper, we report the spectroscopy system in the discharge and magnetic filter areas to investigate Cs behavior inside a  $H^-$  ion source. We have observed a considerable increase in optical emission from neutral Cs in the magnetic filter area. Experimental beam extraction lasting 20 s has been carried out to observe Cs behavior inside the  $H^-$  ion source.

## 2. Optical Configuration of the $H^-$ Ion Source

Figure 1 shows a schematic drawing of the optical configuration of the  $H^-$  ion source for the LHD-NBI. The inner size of the arc chamber is 1450 mm in height ( $y$ -axis), 350 mm in width ( $x$ -axis), and 223 mm in depth ( $z$ -axis) that is measured from the PG surface. The grid system consists of the grounded grid (GG), the extraction grid (EG), and the PG, to which a high voltage of  $-180$  kV is applied. Each grid is divided into five segments along the  $y$ -axis. Hydrogen plasma is produced by arc discharge with 24 tungsten filaments located on the side ports of the arc chamber at  $z = 106$  mm. Cs vapor is supplied from the three Cs ovens installed on the back plate to enhance production of  $H^-$  ions.

Two lines of sight (LOS) exist parallel to the PG in the arc chamber. We have arranged LOS-A on the upper view port located at  $z = 106$  mm to observe the optical emission spectrum in the discharge region. LOS-A views the plasma vertically along the  $y$ -axis, and here we assume an optical integral length of 1.2 m, corresponding to that of the dis-

author's e-mail: ikeda.katsunori@lhd.nifs.ac.jp

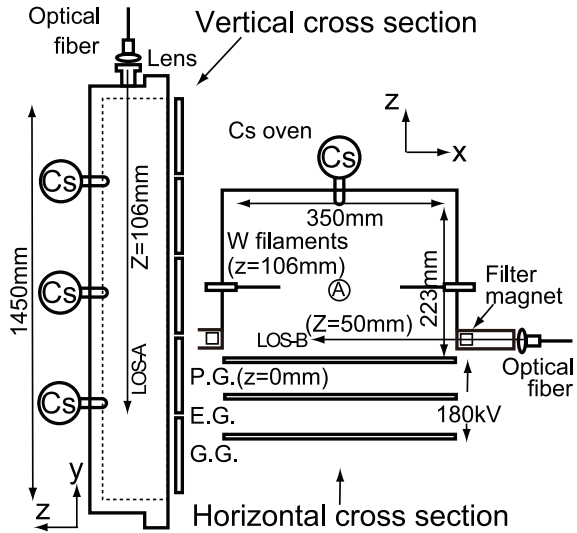


Fig. 1 Schematic view of the optical configurations in the  $H^-$  source for LHD-NBI. LOS-A and LOS-B measure optical emission in the discharge and magnetic filter areas, respectively.

charge region. LOS-B is arranged on the magnetic filter flange at  $z = 50$  mm to observe the magnetic filter region near the PG. LOS-B views the plasma horizontally along the  $x$ -axis, and here we assume an optical integral length of 0.3 m in the magnetic filter region. To measure the hydrogen Balmer spectra ( $H_\alpha$ ,  $H_\beta$ ,  $H_\gamma$ ) and the Cs spectra (Cs I: 852 nm, Cs II: 460 nm), quartz optical fibers coupled with small lenses are used. A wide-range survey spectrometer (PLASUS EmiCon system) is arranged at the opposite side of the optical fibers to take many spectra simultaneously from 200 nm to 870 nm. To compare the optical emission intensity between the two LOS, the spectrometer system is calibrated using an Ulbricht sphere with a standard lamp. Cs densities are estimated by the coefficient rates of the  $Cs^+$  line at 460 nm and the Cs line at 852 nm [8].

### 3. Evolution of the Cs Spectrum in Long Beam Extraction

Cs spectra in the discharge and magnetic filter areas were observed during the 20 s beam operation. Figure 2 (a) shows the time evolution of the arc discharge current ( $I_{arc}$ ) and the acceleration current ( $I_{acc}$ ). The arc discharge voltage was applied from  $t = 6$  s, and  $I_{arc}$  increased to 850 A. After beam extraction from  $t = 17$  s, the  $I_{arc}$  gradually increased to 1050 A because of an increase in the thermal electron emission from the tungsten filaments, which were heated by the back-streaming positive ions. The average arc discharge power ( $P_{arc}$ ) is 78 kW during beam extraction.  $I_{acc}$  was stable around 17 A with a beam energy of 111 keV. Figure 2 (b) shows the time evolution of the hydrogen Balmer- $\gamma$  emission ( $H_\gamma$ ) in the discharge and magnetic filter areas. The  $H_\gamma$  intensities and arc discharge current were stable during beam extraction.

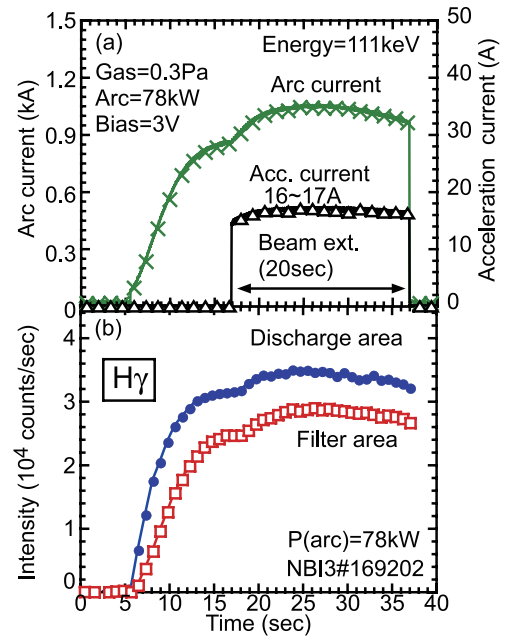


Fig. 2 (a) Development of the arc discharge power (crosses) and acceleration current (triangles) during 20 s beam operation. (b) Development of the  $H_\gamma$  emission intensities in the discharge and magnetic filter areas.

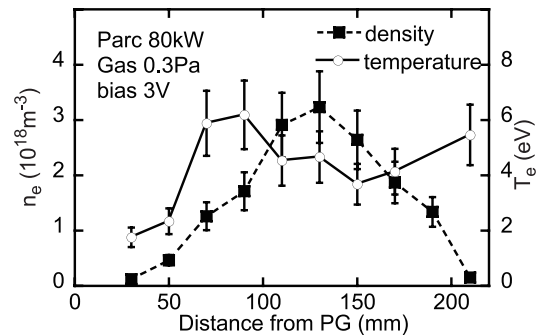


Fig. 3 Temporal profiles of  $n_e$  and  $T_e$  along the  $z$ -axis in 80 kW arc discharge.  $n_e$  and  $T_e$  decrease near the PG because of the magnetic filter field.

Since no electrostatic probe measurement was applied in the beam extraction experiment, the electron density ( $n_e$ ) and the electron temperature ( $T_e$ ) measured in experiments with only arc discharge of the same arc discharge power (80 kW) [10] were used as a reference. From this result, shown in Fig. 3,  $T_e$  and  $n_e$  are estimated at about 5 eV and  $3 \times 10^{18} \text{ m}^{-3}$  at the LOS-A position.  $T_e$  and  $n_e$  decreased to 2 eV and  $0.5 \times 10^{18} \text{ m}^{-3}$  at the LOS-B position because of the magnetic filter field. Since the arc discharge power and  $H_\gamma$  intensity were stable in the 20 s beam experiment,  $T_e$  and  $n_e$  are considered to be stable during beam extraction.

Here, we have estimated the Cs density using the emission rate coefficient ( $X^{Cs}$ ) of the Cs spectrum reported in [8]. The spectrum intensity ( $\epsilon^{Cs}$ ) is expressed as

$$\epsilon^{Cs} = n_e N_{Cs} X^{Cs}(T_e), \quad (1)$$

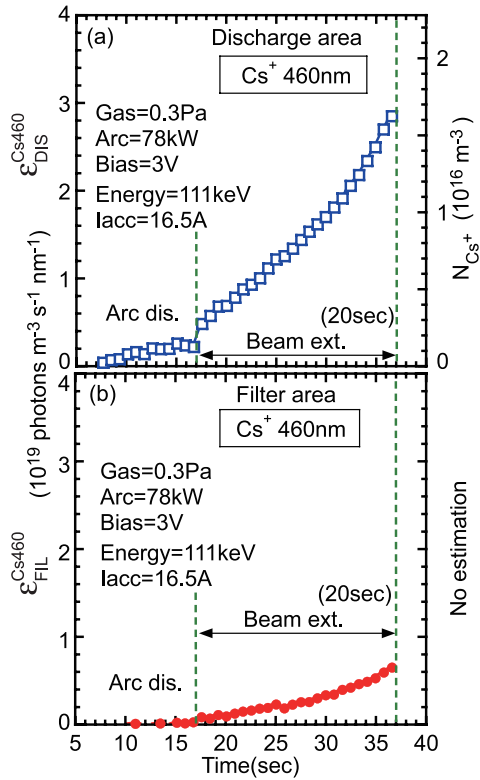


Fig. 4 Evolution of the optical emission of Cs II ( $\lambda = 460$  nm) in the (a) discharge area, and (b) magnetic filter area during 20 s beam operation. The emission rate coefficient of Cs II at 460 nm from [8] is used. The Cs ion density is not estimated in the filter area because the rate coefficient  $X^{\text{Cs}460}$  diminished considerably at  $T_e < 3$  eV.

where  $n_e$  and  $N_{\text{Cs}}$  are the electron density and Cs density, respectively. Thus, the Cs density can be estimated from  $n_e$ ,  $X^{\text{Cs}}(T_e)$ , and the absolutely calibrated  $\epsilon^{\text{Cs}}$ . For the neutral Cs spectrum of Cs I at 852 nm,  $X^{\text{Cs}852}$  was calculated [11] by a quantitative analysis based on the corona model using the electron impact excitation cross sections for Cs I [12]. We use the rate coefficient  $X^{\text{Cs}852} = 9.6 \times 10^{-13} \text{ m}^3 \text{ s}^{-1}$  for  $T_e = 2$  eV, and  $X^{\text{Cs}852} = 1.4 \times 10^{-12} \text{ m}^3 \text{ s}^{-1}$  for  $T_e = 5$  eV. For the ionized Cs spectrum of Cs II at 460 nm, the rate coefficient was not calculated using only quantitative analysis because of the high excitation energy ( $\sim 16$  eV).  $X^{\text{Cs}460}$  was estimated [8] by the Born calculation and approximation analysis using the rate coefficient of the neutral Ar spectrum of Ar I at 750 nm, which has a similar electronic configuration and threshold energy. The rate coefficients of Cs II are  $X^{\text{Cs}460} = 7.4 \times 10^{-18} \text{ m}^3 \text{ s}^{-1}$  for  $T_e = 2$  eV, and  $X^{\text{Cs}460} = 5.8 \times 10^{-16} \text{ m}^3 \text{ s}^{-1}$  for  $T_e = 5$  eV, but these values are uncertain by a factor of 3. In addition, since the  $X^{\text{Cs}460}$  diminished considerably at  $T_e < 3$  eV, we did not estimate the Cs ion density using  $X^{\text{Cs}460}$  in the magnetic filter area.

Figures 4 shows the evolution of the optical emission intensities from  $\text{Cs}^+$  ions in the discharge area ( $\epsilon_{\text{DIS}}^{\text{Cs}460}$ ) along LOS-A and in the magnetic filter area ( $\epsilon_{\text{FIL}}^{\text{Cs}460}$ ) along LOS-B. The spectrum from  $\text{Cs}^+$  was clearly observed in

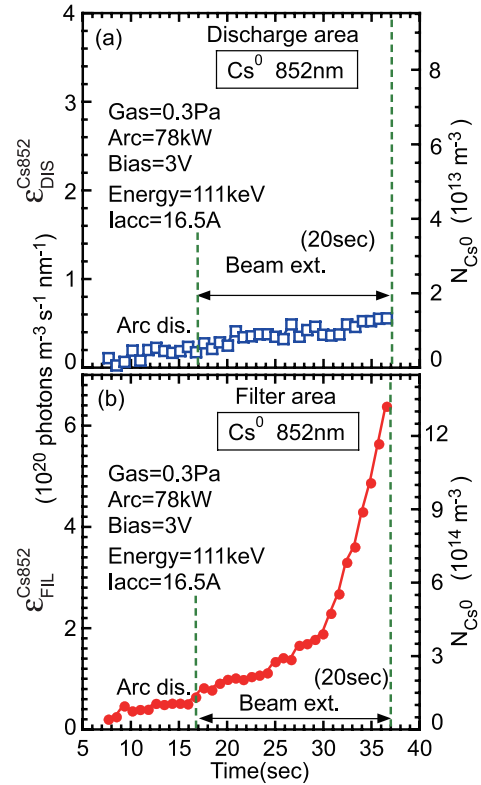


Fig. 5 Evolution of the optical emission of Cs I ( $\lambda = 852$  nm) in the (a) discharge area, and (b) magnetic filter area during 20 s beam operation. The emission rate coefficient of Cs I at 852 nm from [8, 11] is used.

the discharge area, and the influence of back-streaming positive ions on the spectrum intensity was not saturated during long beam extraction, as shown in Fig. 4(a). The increase in  $\text{Cs}^+$  ions caused by the back-streaming ions was 15 times greater than that caused by arc discharge only through evaporation. The  $\text{Cs}^+$  density was two orders of magnitude less than the  $n_e$ . In the filter area, the spectrum from  $\text{Cs}^+$  was not observed in this system with only arc discharge, it increased during beam extraction, as shown in Fig. 4(b). However, the spectrum intensity was very weak, similar to the signal intensity from impurities at 458 nm, because of the low rate coefficient in the filter area. We believe  $\text{Cs}^+$  ions are increased in the filter area as much as in the discharge area by the back-streaming effect. A more careful experiment using an electrostatic probe to measure  $n_e$  and  $T_e$ , and a high-resolution spectrometer for Cs II observation in the filter area is needed.

Figure 5 shows the evolution of the optical emission intensities from Cs neutrals in the discharge area ( $\epsilon_{\text{DIS}}^{\text{Cs}852}$ ) along LOS-A and in the magnetic filter area ( $\epsilon_{\text{FIL}}^{\text{Cs}852}$ ) along LOS-B. In the discharge area, the Cs neutral signal increased slowly even during beam extraction, as shown in Fig. 5(a). The Cs neutral density was less than 1% of the ion density at the end of beam extraction. On the other hand, in the magnetic filter area,  $\epsilon_{\text{FIL}}^{\text{Cs}852}$  increased greatly during beam extraction, as shown in Fig. 5(b). The Cs

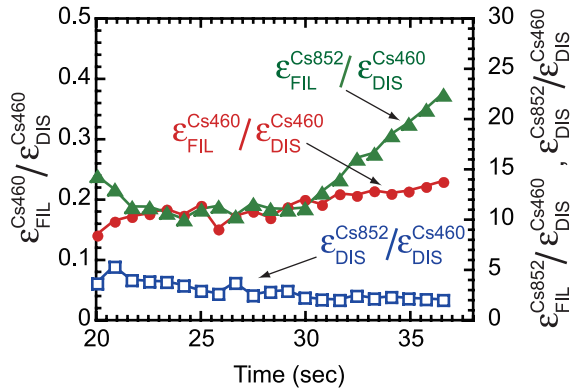


Fig. 6 Development of the Cs spectrum intensity ratio normalized by Cs ion spectrum intensity in the discharge area ( $\epsilon_{\text{DIS}}^{\text{Cs460}}$ ).  $\epsilon_{\text{FIL}}^{\text{Cs460}}$  is almost proportional to  $\epsilon_{\text{DIS}}^{\text{Cs460}}$ . The ratio of  $\epsilon_{\text{FIL}}^{\text{Cs852}}/\epsilon_{\text{DIS}}^{\text{Cs460}}$  is much enhanced after  $t = 30$  s. The ratio of  $\epsilon_{\text{DIS}}^{\text{Cs852}}/\epsilon_{\text{DIS}}^{\text{Cs460}}$  decreases gradually during beam extraction.

density at the end of beam extraction was more than 10 times than that before beam extraction. At around  $t = 30$  s, the rate of increase of neutral Cs was much enhanced in the filter region. Since the rate coefficients of Cs I in the filter and discharge areas are at the same level, Cs neutrals increased significantly only in the filter area. Cs neutrals could enter the discharge area but were immediately ionized there because the ionization energy for Cs (3.89 eV) is lower than the electron temperature.

The development of the Cs spectrum intensities normalized by the  $\epsilon_{\text{DIS}}^{\text{Cs460}}$  intensity are shown in Fig. 6. The intensity of  $\epsilon_{\text{FIL}}^{\text{Cs460}}$  was almost proportional to  $\epsilon_{\text{DIS}}^{\text{Cs460}}$  (circles in Fig. 6). The main source for the increase in  $\text{Cs}^+$  in both the areas was most likely the same, and it is ascribed to heat loading of back-streaming  $\text{H}^+$ . The ratio of  $\epsilon_{\text{DIS}}^{\text{Cs852}}/\epsilon_{\text{DIS}}^{\text{Cs460}}$  decreases slowly during beam extraction. It is suggested that the rate of increase of Cs neutrals is less than that of ions in the discharge area. Evaporated Cs might enter the plasma from the back plate as ions rather than as neutrals. Before  $t = 27$  s,  $\epsilon_{\text{FIL}}^{\text{Cs852}}/\epsilon_{\text{DIS}}^{\text{Cs460}}$  was constant, but it was much enhanced after  $t = 30$  s. This suggests that different Cs sources appeared inside the arc chamber. After the beam experiments, much adsorbed Cs was observed on cooled regions such as the PG support flange and the magnetic filter flange with a water-cooling channel inside the arc chamber. This Cs might evaporate during long pulse operation because of the heat load from the arc discharge.

## 4. Conclusion

The Cs recycling scenario in a negative ion source is believed to consist of three stages. In the first stage with arc discharge until  $t = 17$  s, Cs on the arc chamber wall evaporates because of the heat load from the arc discharge

and enters the plasma. Evaporation of Cs from the chamber wall and the loss of Cs to the cooled regions on the arc chamber surface are balanced. At the second stage, after beam extraction ( $t = 17 \sim 30$  s), Cs on the back plate is evaporated by back-streaming  $\text{H}^+$  ions, and most of the Cs in the discharge region is ionized. Cs neutrals in the filter region also increases because of the back-streaming effect. In these two stages, the Cs loss regions are the cold surfaces of the chamber wall, and most of the Cs would not be recycled during short beam operation. At the third stage, in the long beam extraction at  $t > 30$  s,  $\text{Cs}^+$  ions from the back plate still increase without saturation and enter the plasma. Cs evaporation from the loss regions of the chamber wall begins because of the heat load due to the long arc discharge; the Cs enters the filter region near the PG. The rate of increase of neutral Cs caused by long arc discharge is larger than that caused by back-streaming.

In a negative ion source, positive Cs ions cannot enter the grid region because of the potential barrier of the extraction and acceleration voltages. Cs neutrals, however, can enter the grid system by passing through the holes in the grid. We have not observed degradation of the voltage holding in short-pulse operation. However, the increase in Cs neutrals near the PG might be a more important issue for long-pulse, high-power operation in future NBIs.

## Acknowledgement

The authors thank the NBI staff for their operational support. We also thank Professor U. Fantz (Max-Planck-Institut für Plasmaphysik) for useful discussions. This work was supported by the budget for NIFS09ULBB701.

- [1] M. Kuriyama, N. Akino, N. Ebisawa *et al.*, J. Nucl. Sci. Technol. **35** (11), 739 (1998).
- [2] Y. Takeiri, O. Kaneko, K. Tsumori *et al.*, Nucl. Fusion **46**, S199 (2006).
- [3] E. Speth, H. D. Falter, P. Franzen *et al.*, Nucl. Fusion **46**, S220 (2006).
- [4] R. S. Hemsworth, A. Tanga and V. Antoni, Rev. Sci. Instrum. **79**, 02C109 (2008).
- [5] K. Ikeda, K. Nagaoka, Y. Takeiri *et al.*, Plasma Science and Technology **11** (4), 452 (2009).
- [6] Y. Takeiri, O. Kaneko, K. Tsumori *et al.*, Rev. Sci. Instrum. **71** (2), 1225 (2000).
- [7] D. Marcuzzi, M. Dalla Palma, M. Paveia *et al.*, Fusion Eng. Des. **84**, 1253 (2009).
- [8] U. Fantz, H. Falter, P. Franzen *et al.*, Nucl. Fusion **46**, S297 (2006).
- [9] K. Ikeda, K. Nagaoka, Y. Takeiri *et al.*, Rev. Sci. Instrum. **79**, 02A518 (2008).
- [10] K. Ikeda, U. Fantz, K. Nagaoka *et al.*, Plasma Fusion Res. **2**, S1047 (2007).
- [11] U. Fantz, H. D. Falter, P. Franzen *et al.*, Fusion Eng. Des. **74**, 299 (2005).
- [12] P. S. Ganas, J. Chem. Phys. **76**, 2103 (1982).